Hindawi Publishing Corporation
International Journal of Distributed Sensor Networks
Volume 2012, Article ID 310797, 10 pages
doi:10.1155/2012/310797

Research Article

Application of Multiscale Fiber Optical Sensing Network Based on Brillouin and Fiber Bragg Grating Sensing Techniques on Concrete Structures

Xuefeng Zhao,[1] Jie Lu,[2] Ruicong Han,[1] Xianglong Kong,[1] Yanhong Wang,[1] and Le Li[1]

[1] *School of Civil Engineering, Dalian University of Technology, Dalian 116024, Liaoning, China*
[2] *Structural Design Center, The Fifth Research Design Institute of Nuclear Industry, Zhengzhou 450052, Henan, China*

Correspondence should be addressed to Xuefeng Zhao, zhaoxf@dlut.edu.cn

Received 19 June 2012; Accepted 27 August 2012

Academic Editor: Ting-Hua YI

The paper reports the application of the distributed optical fiber sensing technology and the FBG sensing technology in bridge strain monitoring; the overall changeable characteristics of the whole structure can be obtained through the distributed optical fiber sensing technology (BOTDA), meanwhile the accurate information of local important parts of the structure can be obtained through the optical fiber Bragg grating sensor (FBG), which can improve the accuracy of the monitoring. FBG sensor has a high sensitivity, but it can only realize the measurement of local discrete points for the quasidistributed sensing. BOTDA can realize the long distance and distributed measurement, but its spatial resolution is not high. FBG and BOTDA were applied together in bridge monitoring in this test, taking full advantage of the distributed BOTDA on the overall strain measurements of the structure, as well as monitoring the key parts by the arrangement of FBG. The combined application of BOTDA and FBG can achieve the overall monitoring from point to line and then to the surface and, therefore, obtain more comprehensive information on the strain of the test structure.

1. Introduction

In china, with the continuous construction of large-scale infrastructure projects and facilities, the technology of the construction quality monitoring under construction and the health diagnosis in structural service are increasingly required. A key issue in structural health monitoring is how to monitor, identify, locate, and calibrate the force in the structural system effectively. Some researchers studied the optimal sensor installation method, in order to make the sensor networks work more efficiently. Li et al. and Yi et al. have systematically studied this issue proposed some meaningful optimal sensor installation methods and algorithms [1–4]. Brillouin optical time-domain analysis technology (BOTDA) is a distributed optical fiber strain sensing technology based on stimulated Brillouin backscatter principle, which breaks through the traditional concept of point sensing and realizes the continuous distributed monitoring in its true sense. The sensing gauge and the spatial resolution in the temperature and strain measurement can reach a higher level than other sensing technologies. So BOTDA has become a high-end sensing technology in the large civil engineering health diagnosis, which leads to the international advanced developed countries race to research. Scholars have been doing some research and applications on this technology. Xuan et al. had applied BOTDA technique to monitor the strain of reinforced concrete structure for monitoring steel bar corrosion according to the variation of strain distribution [5]. Qian et al. monitored the cracking development for asphalt concrete pavement [6]. He et al. studied the real-time reinforcement stress measurement ability of BOTDA technique [7]. FBG (fiber bragg grating) is a new type of optical components. Due to the higher monitoring accuracy and the mature technology, it has

been widely used in the monitoring of large structures. Sun reported the application in civil engineering systematically [8]. And other researchers had developed a monitoring technique for various parameters detection using FBG sensing technique [9–11]. Distributed fiber optic sensors have more advantages compared with conventional sensing methods as follows. Firstly, the measured spatial distribution state and time-varying information can be obtained simultaneously; secondly, FBG provides continuous measurement of the fiber environment parameters along the entire fiber; thirdly, theoretically the measured information can be a function of the fiber position, resulting in obtaining the resolution of any size; lastly, it is feasible to use an optical fiber to replace the traditional sensors array which consists of hundreds of dot matricies, which greatly reduce the cost of monitoring. FBG monitoring accuracy is high, but the cost is expensive; besides, the measuring point is relatively independent, and it is difficult to grasp the overall variation law of the structure. So it is reasonable to combine the two monitoring tools, combining distributed optical fiber and FBG, together with the structure, making full use of the advantages and avoiding the disadvantages. The distributed optical fiber sensors and FBG are used in the critical part of the structure at the same time to cross-check the two monitoring results. And only the distributed optical fiber sensors are used in the noncritical part of the structure to monitor the general trend of the structure. Experimental results demonstrate the good effect of the joint monitoring.

2. Basic Principle of the Fiber Bragg Gating and BOTDA

2.1. Basic Principle of the FBG. Fiber core is a photosensitive material, that is, the refractive index of the core varies with the intensity of the UV irradiation. Fiber Bragg grating makes use of this photosensitivity. By using this photosensitivity and ultraviolet writing technique to write the coherent field of the incident light to the core, refractive index of the core periodically changes and forms the FBG whose refractive index changes along the fiber length, as shown in Figure 1. The change of grating ambient temperature, strain, stress, or other test physical quantity will result in the change of the core refractive index or the grating period and then result in the wavelength change of fiber Bragg grating signal. By monitoring the changes of the grating wavelength λ_B, the change of physical quantities to be tested can be obtained [9].

Bragg grating center wavelength of the reflected light (Bragg wavelength) is called characteristic wavelength and satisfies

$$\lambda_B = 2n_{\text{eff}}\Lambda, \tag{1}$$

where n_{eff} is refractive index, and Λ is grating period. Equation (1) demonstrates that when n_{eff} alters, λ_B changes accordingly. Through the Bragg grating center wavelength detection, the structure strain and the changes of outside conditions such as temperature can be obtained. In the process of fiber Bragg grating sensor measuring the strain and temperature, the change of strain and temperature will lead to the change of reflected light center wavelength of Bragg grating, and the relationship between the offset of center wavelength and the change of strain and temperature is shown as as follows:

$$\Delta\lambda_B = \lambda_B(1 - \kappa_\alpha)\Delta\varepsilon + \lambda_B(1 + \zeta)\Delta T, \tag{2}$$

where $\Delta\lambda_B$ is the offset of center wavelength of the reflected light, $\Delta\varepsilon$ is the change of strain, ΔT is the change of temperature, κ_α is the elasto-optical coefficient of fiber, and ξ is the thermo-optical coefficient of fiber.

Equation (2) shows that the wavelength of grating has dual sensitivity to the external strain and external temperature; the changes of temperature/strain will lead to changes in the wavelength of fiber Bragg grating sensors, which can be detected from the grating reflection spectrum. By comparing the grating wavelength before and after the motivation, calibrating the offset by the variation of wavelength, then the pressure and the strain values on different points can be obtained.

2.2. The Principle of BOTDA. The basic principle of the Brillouin optical time-domain analysis (BOTDA) is based on the feature of Brillouin-stimulated amplification. The spontaneous Brillouin scattering intensity increases as the pump light intensity increases, and when the intensity reaches a certain extent, the reverse transfer Stokes light and pump light will interfere, causing strong interference fringes, then the fiber-optic local refractive index greatly increases. Because of electrostrictive effect, it will produce acoustic waves, which inspire more Brillouin-scattered light, and the inspired scattered light also enhances the acoustic wave at the same time, and the interactions produce a very strong scattering, which is stimulated Brillouin-scattering (SBS) [12], as shown in Figure 2.

The value of Brillouin frequency shift is given by

$$\nu_B = \frac{2n\nu_a}{\lambda_0}, \tag{3}$$

where ν_B is a Brillouin frequency shift, n is the refractive index of the fiber core, ν_a is the acoustic velocity, and λ_0 is the wavelength of incident light in vacuum. For common silica glass fibers, $n = 1.46, \nu_a = 5945\,\text{m/s}$, when $\lambda_0 = 1550\,\text{nm}, \nu_B = 11.2\,\text{GHz}$.

The Brillouin frequency shift of the incident light ν_B is related to the fibers' temperature and the strain ε; the relationship between them is shown as follows:

$$\nu_B(\varepsilon, \theta) = \nu_B(0, \theta_0) + \frac{\partial\nu_B}{\partial\varepsilon} \cdot \varepsilon + \frac{\partial\nu_B}{\partial\theta}(\theta - \theta_0), \tag{4}$$

where $\nu_B(\varepsilon, \theta)$ is the Brillouin frequency shift when the fiber strain is ε under the temperature θ, $\nu_B(0, \theta_0)$ is the Brillouin frequency shift under θ_0 when the fiber strain is zero, $\partial\nu_B/\partial\varepsilon$ is strain coefficient, $\partial\nu_B/\partial\theta$ is the temperature coefficient, θ_0 is reference temperature, and ε is the fiber strain.

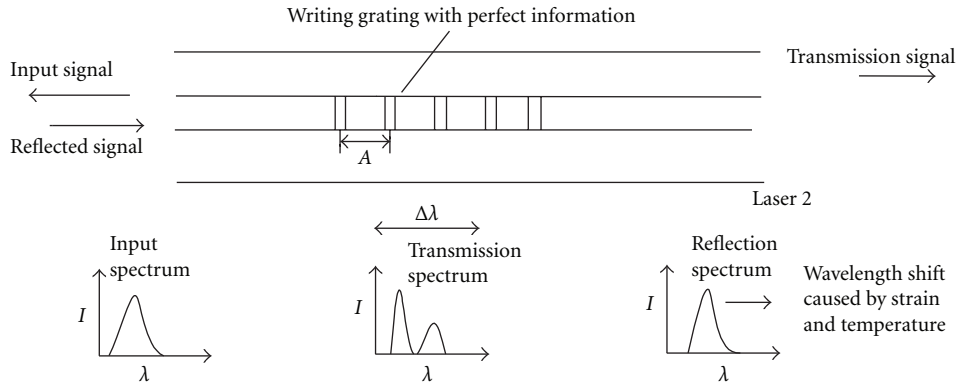

Figure 1: Schematic drawing of ultraviolet reads grating.

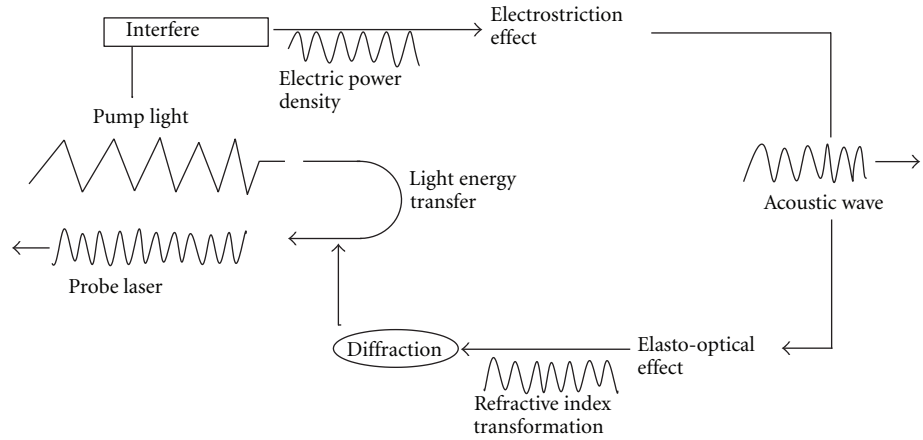

Figure 2: Stimulated Brillouin scattering produce process.

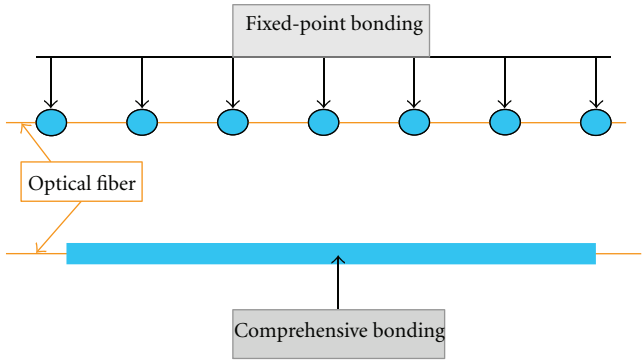

Figure 3: The pattern of laying method.

3. The Laying Method of Distributed Fiber and FBG

Two methods are used to lay distributed optical fiber sensor. One is comprehensive bonding, that is, the fiber optic sensor sensing area is fully bonded to the structure, whose characteristic is realizing an overall monitoring to the structure deformation; this kind of bond needs a specific placing technology; distributed optical fiber sensors and Bragg grating sensors are bounded to the structure surface according to the design route with an effective binder; then connecting the sensing fiber end to the monitoring instruments, the monitor signal will be fed back to the monitoring system through the optical fiber. Another way is the fixed-point contact laying, that is, the paste point is determined at intervals of 1 m or 2 m along the optical fiber and then pasted to the monitoring body, and the measured strain value is the average strain value between the pasted points. This method is always used on the distortion position, and usually the space distance between the fixed points is greater than the spatial resolution of BOTDA. The fixed-point contact laying method is roughly equivalent to the comprehensive contact laying method, but the difference is to select some point on the designed construction surface to bond. Figure 3 illustrates the schematic of comprehensive bonding and fixed-point contact. Different methods should be adopted to lay the monitoring optical fiber in actual application according to the structural characteristics and monitoring purpose.

In order to meet the monitoring requirements on different sizes, fixed-point contact laying method is adopted to increase the measuring range of the fiber Bragg grating

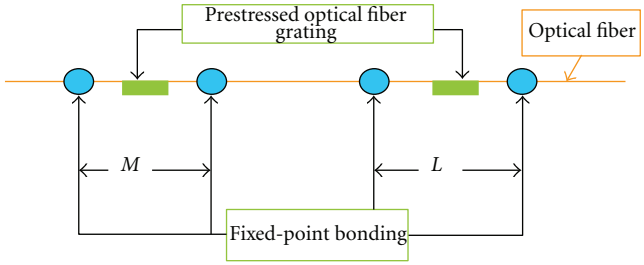

Figure 4: The way of pc FBG adhesive in different distance.

sensors, and FBG monitoring strain is the average strain between the two pasted points. In order to ensure that the fiber grating can monitor effectively, preload tensile stress of 300–400 microstrain to the grating to prevent grating relaxation, which will lead to monitor failure or get wrong monitoring results. Figure 4 gives the paste way of prestress FBG in different distance.

4. Experiment Introduction

4.1. Test Beam. This experiment is located in Development Zone of Zhenliang Road in Dalian. The length of the bridge is 2817.004 m (k7 + 080 K9 ~897.004), the width of single-standard cross-section of mainline bridge is 23.5 m; the section of the superstructure is single box and multicell. Of all the prestressed continuous concrete beam, in addition to the height of special-shaped beam is 1.6 m, the height of other beams and cantilever is 1.5 m. The thickness of the web in the midspan and the fulcrum position is 0.4 m and 0.6 m, respectively. Most of the bridge superstructure is a prestressed structure, which forms multiple prestressed concrete box girder connection, so isolation joint pouring is used, and wet joint pouring is used for the remaining joints in the construction sequence. The cross-slope of deck is adjusted by the cross-slope of coping flange plate.

The test bridge is located in a straight line segment, and beam length is 30 m. Superstructure is the simply supported transgenic continuous structure with prestressed concrete box girder. Substructure is the piers with circular cross-section, piers that match with different forms of the pier cap and the capping beams according to the superstructure. The capping beams are prestressed structures, whose cross-sections are small and in a beautiful form. Bearing plate bed is set on the top of part of the pipers. Bored pile is used in pipe foundation. Figure 5 shows the cross-section of beam.

According to the construction drawings provided by the commissioning party, the load under the ultimate limit state is equivalent to the uniformly distributed load according to the Highway Bridge Design General specification (Take the deadweight of the beam, deck pavement, vehicle load, and other loads into consideration. The worst load transversal distribution coefficient is 0.63, and the load effect combination is done combined under the limit state.). The design load is 130 tons. During the test, give the bending moment of the midspan as the control loading, and the load is equivalent to the uniformly distributed load; in the test, the maximum load of the beam is 87 tons.

4.2. The Scheme of Multiscale FBG Network. The arrangement of distributed optical fiber sensors and FBG along the T-box girder flange was shown in Figures 6 and 7. Theoretical analysis shows that the axial strain of simply supported beam is larger than other directions. The laying of monitoring optical fiber mainly measures the axial strain, so one-dimensional network is used, and the comprehensive bonding method was adopted to arrange the optical fiber along the beam length direction, and 20 m free optical fiber was reserved as a temperature sensor at the beam end. Five fiber-optic temperature sensors were set up on the beam for temperature compensation, and distributed fiber-optic sensor network was shown in Figure 6. Distributed optical fiber strain sensors connected to the BOTDA were divided into five regions which, respectively, are S1, S2, S3, S4, and S5; distributed optical fiber temperature sensors respectively were T1, T2, T3, T4, and T5. Three flexometers were placed at beam bottom, on fulcrum position, and midspan of the beam, respectively. Distributed optical fibers were fixed with 502 glue at the interval 1-2 m firstly and then were bonded comprehensively with the AB glue. The optical fiber needs to be tested with optical power meter or light source so as to check the on-off and loss of the optical fiber, then inspect and repair the abnormal point, and weld the breakpoint. In order to obtain better measurements and eliminate the end effect, a length of fiber should be set aside at both ends, generally greater than 50 m.

The fiber Bragg grating strain sensors on the beam were named as follows: L31, L32, L33, L34, and L35, and in order to increase the measurement range of FBG, two points pasting method were adopted, applied prestress about 200–300 microstrain on two paste points, and then fixed the two points with AB glue. L31, L32, and L33 were preloaded grating sensors, and the length is 30 cm. The strain measured by FBG is the average strain in the range of 30 cm; L33, L34, and L35 are directly attached to the beam, in which gauge length is 10 cm.

FBG was mainly arranged in the parts where force is considerable, such as the bottom of the midspan and quarter span of the structure. The arrangement of FBG was shown in Figure 7. Put more than one grating sensor in series, and use quasidistributed measurement to reduce the measurement workload. But it needs to be paid attention to distinguish different sensors in advance according to the wavelength before laying out FBG, and the wavelength of the sensors put in a line must contain certain interval, otherwise the instrument cannot recognize or distinguish the measurement points.

4.3. Data Acquisition System. The main instruments and equipment used in the experiment are as follows: BOTDA (STA100), fiber cleaver, fiber fusion splicer (FSM-50S), thermostatic bath (DC-2015), hot pyrocondensation pipe, fiber grating, weights, computer, multichannel fiber-optic grating demodulator (TFBGD-9000), fiber, and so forth. The

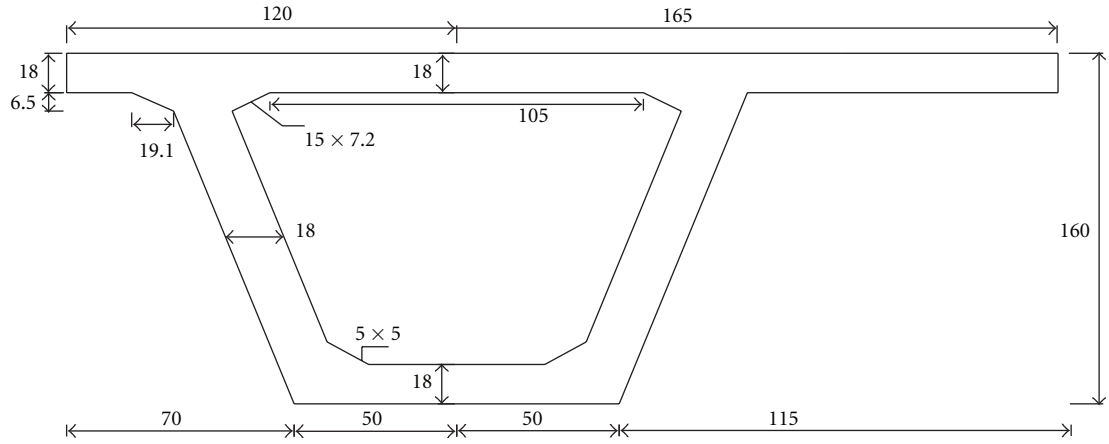

Figure 5: Cross-section of beam (unit: cm).

Table 1: BOTDA STA 100 performance index.

Type	STA 100-C	Maximum number of measurement point	100000
Sensing structure	Loop	Measurement average	1~10000
Channel	2	Optical fiber connector	FC-APC (E-2000)
Spatial resolution	0.5~20 m	Laser wavelength	1550 nm
Range resolution	0.2 m	Sampling time	20 s (1-2 min)
Range of strain	−1.5%~1.5%	Temperature range	−270~700°C

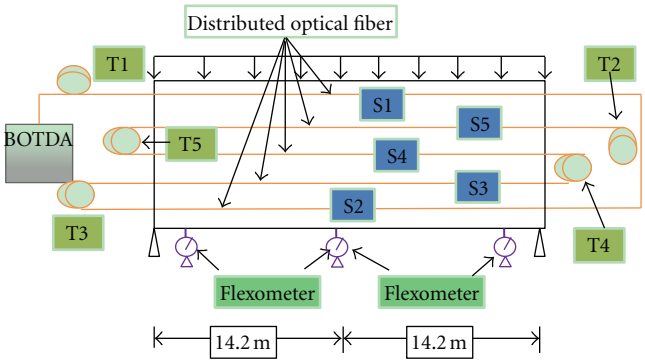

Figure 6: Beam diagram of optical fiber sensor network.

Figure 8: BOTDA (STA100).

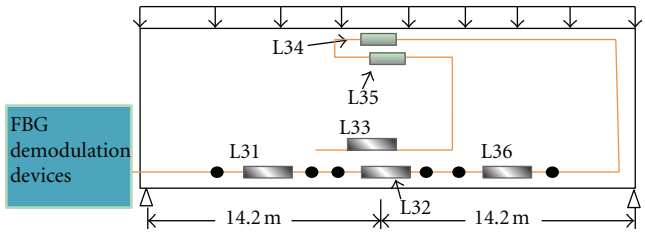

Figure 7: Beam diagram of FBG network.

following mainly describes the basic parameters of the experimental fiber, the main performance indicators of Brillouin optical time-domain analysis instrument BOTDA (STA100), and multichannel fiber Bragg grating demodulator (TFBGD-9000).

(i) The introduction of BOTDA (STA100): the Institute of the Smart Structural Systems in Dalian University of Technology imported the BOTDA (STA100) from Switzerland. The appearance of BOTDA is shown in Figure 8, and the performance indicators are shown in Table 1; the basic features are showed as follows:

(1) distributed temperature, strain measurements, and long-distance measurement which can be up to 30 km;

(2) high spatial resolution, long-term stability, and reliability;

Table 2: TFBGD-9000 fiber grating demodulation devices performance indicator.

Optical channel	16~64 (can be extended arbitrarily)	Wavelength range	1520~1570 NM
Wavelength resolution	1 PM	Repeatability	2 PM
Scanning frequency	300 HZ (can be set by software)	Power supply mode	220 V AC
Data storage method	USB	Communication interface	Ethernet, RS-232, USB

Table 3: Numerical solution of beam.

Location	Load		
	4.986 KN/m^2	7.978 KN/m^2	9.97 KN/m^2
Quartile	131 ($\mu\varepsilon$)	162 ($\mu\varepsilon$)	183 ($\mu\varepsilon$)
Midspan	180 ($\mu\varepsilon$)	223 ($\mu\varepsilon$)	252 ($\mu\varepsilon$)
Quartile	131 ($\mu\varepsilon$)	163 ($\mu\varepsilon$)	184 ($\mu\varepsilon$)

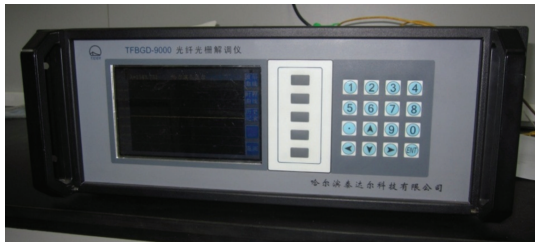

Figure 9: TFBGD-9000 grating demodulation device appearance.

(3) strain accuracy: 20 $\mu\varepsilon$ (0.002%), temperature accuracy: 1°C;

(4) measurement modes: manual or automatic measurement;

(5) data analysis: measurement, analysis, comparison of multiple data analysis, and graphical zoom.

(ii) The introduction of multichannel fiber Bragg grating demodulator (TFBGD-9000): the instrument adopts a high-power scanning laser light source, which is suitable for distributed monitoring of large-scale projects; there is no need for expensive optical switch devices, and which can achieve multichannel synchronous acquisition in the true sense. It uses parallel data processing algorithm, and there is no delay between the channels, so it has excellent dynamic performance; channel scalability is extremely high, which can extend to 64 channels easily with a low cost of channel expansion; the scan rate is 300 HZ, so the scan speed can be set by software, meanwhile it can also be compatible with the static work. The fiber optic sensors have a high capacity; 64 channels are available for over 2000 FBG sensors; integration of data acquisition device and optical access module makes the structure simple and easy to install; the appearance; as shown in Figure 9 is the performance/indicators is as shown in Table 2.

4.4. The Test Procedure. The distributed fiber optic strain monitoring system BOTDA was used to test the fiber when optical fiber laying was completed and took the result as the initial value of periodic measurement. Since this experiment was only a short-term measurement, step loading was adopted to collect data. The first load was 43.5 t, the second load was 69.6 t, and the third load was 87 t; the corresponding uniformly distributed loads were 4.986 KN/m^2 , 7.978 KN/m^2, and 9.97 KN/m^2. Each loading lasted for 10 minutes and then was read and recorded after the strain and deformation were stable, after all loads were applied, lasted for 10 minutes was read, and then unloaded and collected data 10 minutes later.

Distributed optical fiber sensor adopted Brillouin optical time-domain analyzer (BOTDA) to collect the data, which is stored in the instrument directly, and only needs to name files. Fiber Bragg grating sensors used fiber Bragg grating strain demodulation devices to collect data which is dynamic acquisition.

5. Numerical Simulation and Analysis

5.1. The Results of Finite-Element Numerical Model. The finite-element model of prestressed box girder was established by the universal finite-element software ANSYS10.0. Solid element was adopted to establish the model. The two ends of the beam are hinge structure, using SOLID95 element, which is more advanced than the 3D 8-node solid elements SOLID45. The y-axis node strain contour under uniformly distributed load (9.972 KN/m^2) is shown in Figure 10. It can be seen from the figure that the pressure of the top of the midspan girder is the largest. The finite strain numerical solution at the bottom of the beam in midspan and quartile with all levels of load is shown in Table 3.

5.2. Distributed Optical Fiber Sensor Monitoring Results. S1 is the distributed strain sensor on the T-box girder flange, S2 is the strain sensor on the bottom of the beam, S3, S4, and S5 are distributed optical fiber sensors distant from the bottom of the beam are 32 cm, 66 cm, and 102 cm respectively, and T1~T5 are distributed optical fiber temperature sensors. The method of temperature compensation on strain sensor is as follows: calculate the temperature of each temperature sensor T1 ~ T5, because the ambient temperature is not uniform, so the average temperature of the five optical fiber temperature sensors can be the temperature compensation of the strain sensor. Figure 11 is monitoring data of the entire

Table 4: FBG strain of beam.

Sensor number	Load			
	4.986 KN/m^2 strain ($\mu\varepsilon$)	7.978 KN/m^2 strain ($\mu\varepsilon$)	9.97 KN/m^2 strain ($\mu\varepsilon$)	Complete unload strain ($\mu\varepsilon$)
L31	73.33	123.33	164.17	5.83
L32	105	173.33	227.5	15
L33	73.33	121.67	156.67	37.5
L34	−20.83	−34.17	−45	25
L35	−14.17	−20.83	−26.67	30.83
L36	84.17	137.5	176.67	10

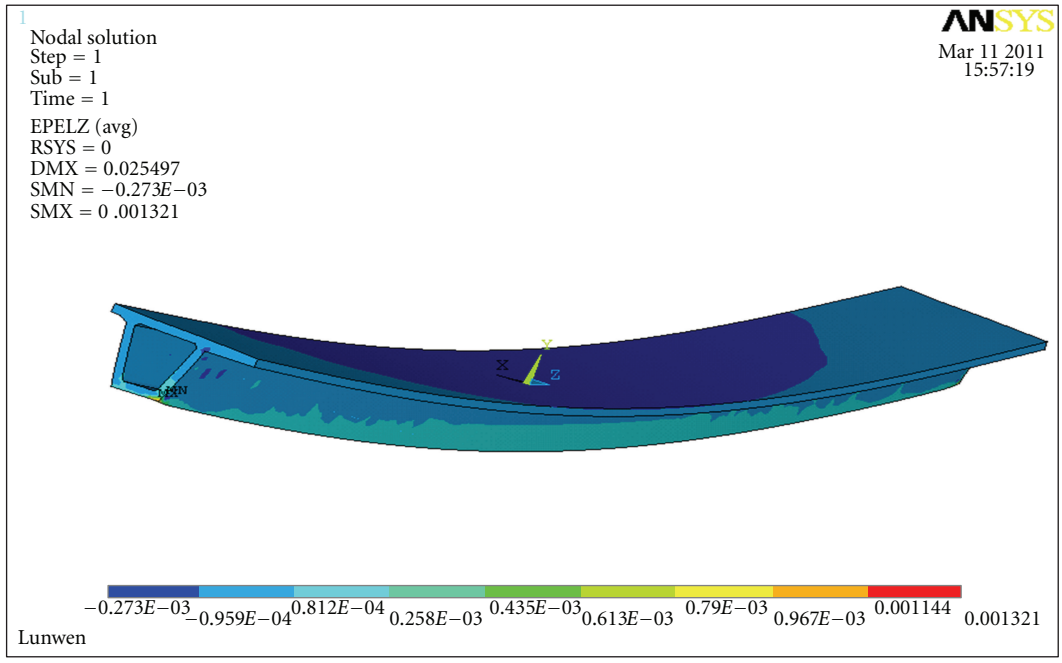

Figure 10: The node of y-axis strain contour.

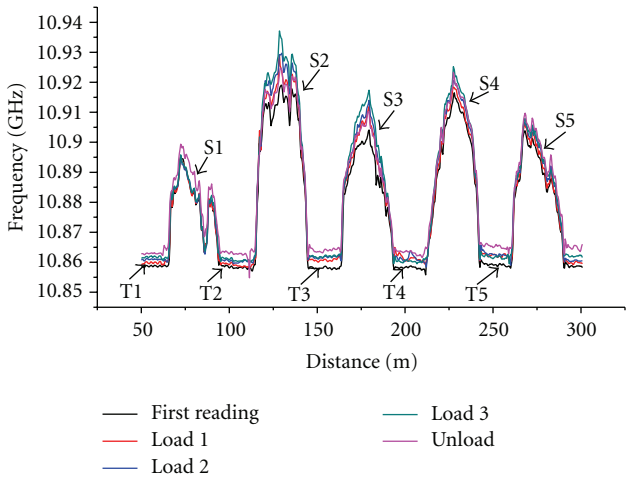

Figure 11: Curve of distributed fiber sensor frequency-distance.

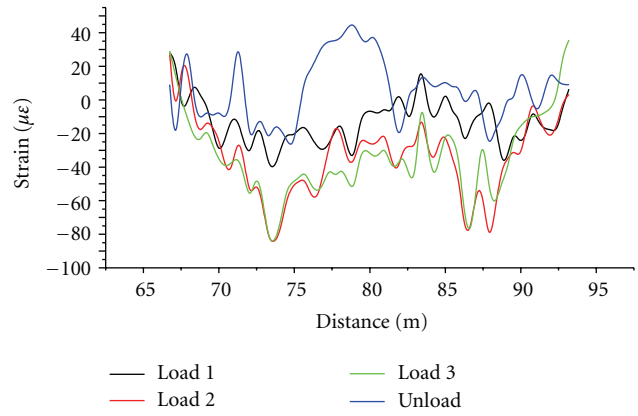

Figure 12: Curve of S1 distributed optical fiber sensor strain-location.

sensor network; the monitoring strain of five distributed optical fiber strain sensors after temperature compensation is as shown in Figures 12, 13, 14, 15, 16.

Figure 12 shows the strain variation of the bottom of box girder flange which is obtained by the monitoring of distributed optical fiber strain sensor S1. Four curves in the figure, respectively, are strain curves after loading three

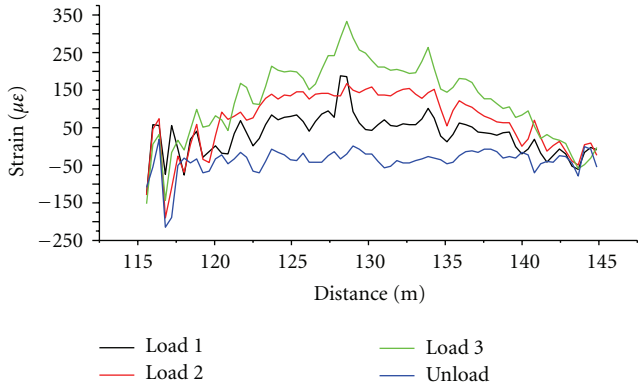

Figure 13: Curve of S2 distributed optical fiber sensor strain-location.

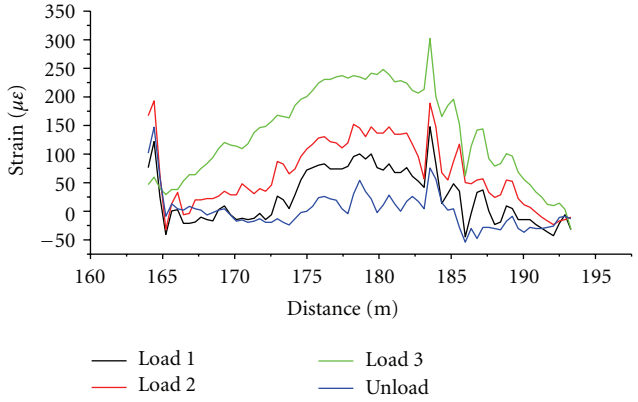

Figure 14: Curve of S3 distributed optical fiber sensor strain-location.

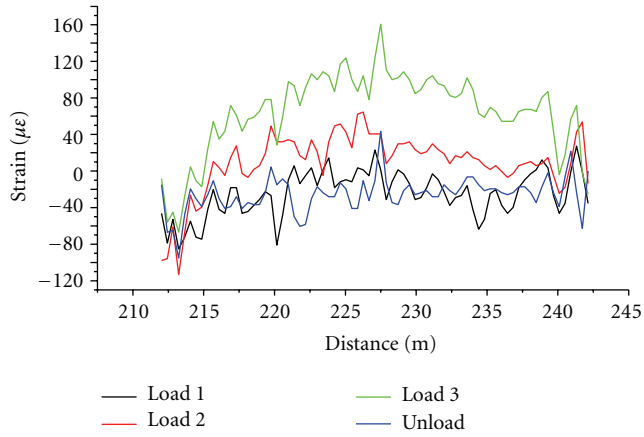

Figure 15: Curve of S4 distributed optical fiber sensor strain-location.

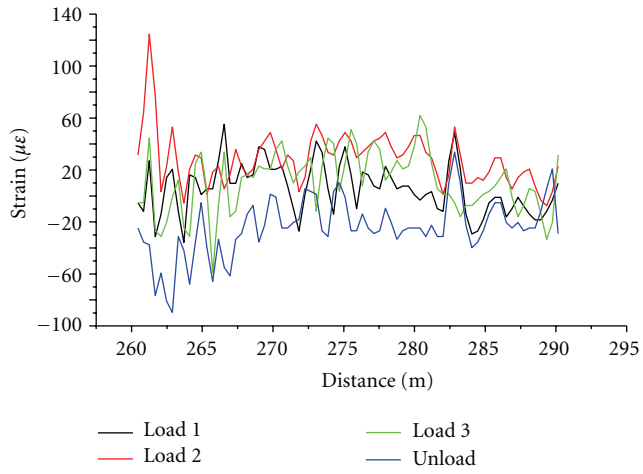

Figure 16: Curve of S5 distributed optical fiber sensor strain-location.

times and unloading, and it can be seen from the figure that the bottom of the beam is compressed; with the load increases, the compressive strain has a trend to increase, but the results of monitoring are not stable. According to the stress characteristics of simply supported beam under uniformly distributed load, the maximum strain occurred in the midspan, but the peak strain of the monitoring result is not in the midspan.

Figures 13–16 show that with the load increases, the strain of the concrete beam increases gradually; with the increase of tensile strain, the measurement results of distributed optical fiber become more and more stable, the peak is apparently in the midspan. Distributed strain measurement results comply with the strain distribution characteristics of simply supported beam under uniformly distributed load, which form a parabolic distribution, gradually increasing from both ends towards the middle.

5.3. FBG Monitoring Data. Corresponding to the measurement points $(l, \ldots, n)$ of the test structure, according to reflection wavelength of different grating, quasidistributed fiber Bragg grating sensors feel the stress and strain of each point along the test structure, respectively, and make the wavelength of the reflected light change; the change reflected light transmitted from the measurement site though the transmission fiber; to detect the change of wavelength with fiber Bragg grating demodulator and convert it into electrical signals, calculate the stress and strain of the points of the test structure and the distribution of the entire test structure by the secondary instrument.

Each grating strain sensor measurement results after temperature compensation calculated are shown in Table 4, and the quasidistributed strain monitoring results of FBG are shown in Figure 17.

5.4. Results Discussion. Figure 18 is a Gauss fitting curve of distributed optical fiber; FBG and ANSYS are numerical solution strain results for the first time loading 4.986 KN/m^2; Figure 19 is a Gauss curve fitting of distributed optical fiber; FBG and ANSYS are numerical solution strain results for the second time loading 7.978 KN/m^2; Figure 20 is a Gauss curve fitting of distributed optical fiber; FBG and ANSYS are numerical solution strain results for the third time loading 9.972 KN/m^2.

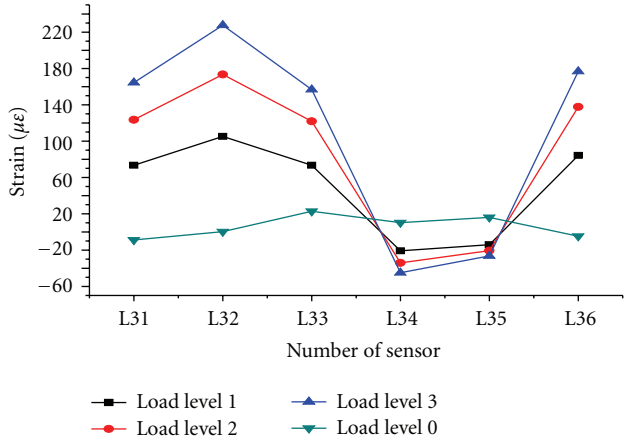

Figure 17: Strain of grating strain sensor after temperature compensation.

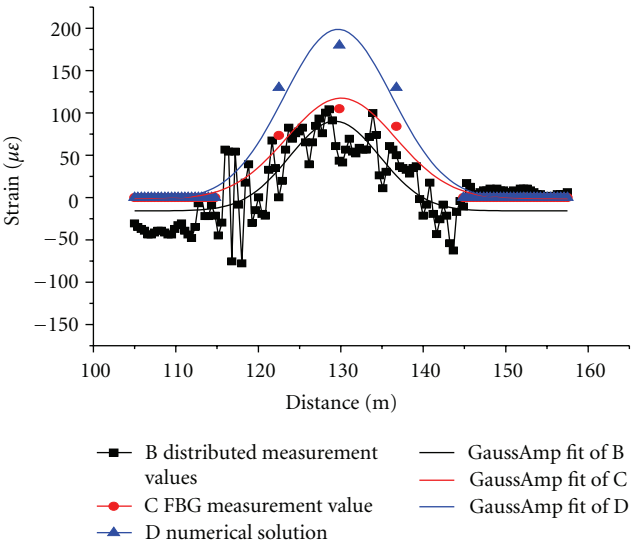

Figure 18: Gauss fitting curve of the load 4.986 KN/m^2.

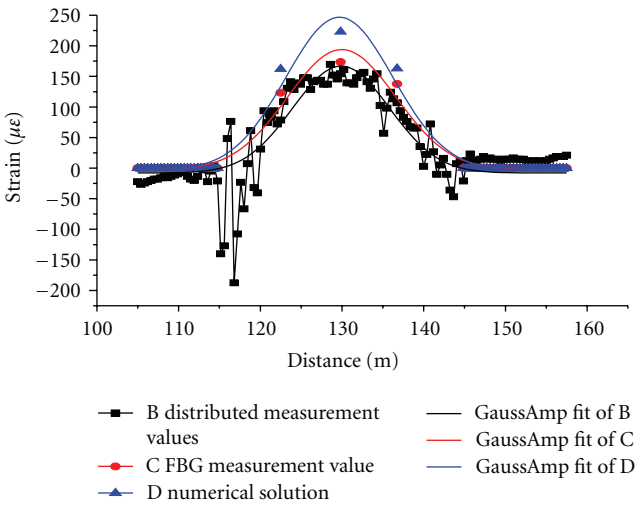

Figure 19: Gauss fitting curve of the load 7.978 KN/m^2.

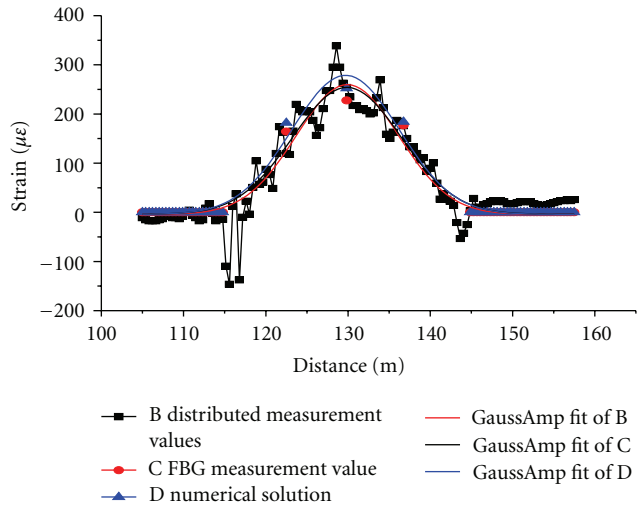

Figure 20: Gauss fitting curve of the load 9.972 KN/m^2.

From the Gauss fitting curve in Figures 18–20, it is concluded that when load and structural strain are small, due to the law strain accuracy of Brillouin optical time-domain analyzer (BOTDA), the deviation between measurement results and theoretical values solution is greater. As the load increases, the distributed measuring results of fiber Bragg grating and numerical simulation solution are closer and closer. When the load was 7.978 KN/m^2, the structural strain was greater than 200 $\mu\varepsilon$, and the fitting curves of monitoring value almost meet FBG measured values and numerical solutions, and the maximum deviation of the fitted values is 7%. It can be also known from the figure that when measuring the small strain, the results of FBG are more accurate than those of the distributed monitoring, but with the increase of load, the results of deviation between distribution strain monitoring and fiber Bragg grating decreased gradually. Because the strain measurement precision of BOTDA is less than FBG's, the BOTDA monitoring result has shown a larger error than FBG's results. And when the load applied increased, the error will become relatively small compared with FBG results. BOTDA is not suitable for monitoring small strains, otherwise there would be a great error. Figure 21 shows the results contrast between BOTDA, FBG, and finite-element numerical solution of the beam bottom. Figure 22 shows the contrast of across-pressure zone strain of distributed optical fiber and FBG; the experiments show that the BOTDA is not suitable for monitoring structure with small compression strain; while as the load increases, the deviation of the monitoring results between the distributed and fiber grating reduces gradually.

6. Conclusion

More comprehensive information of the structure can be obtained by the full-scale distributed optical fiber sensing technology which is easy to capture the overall stress condition of the structure; fiber Bragg grating sensors monitor the local point, get more precise information of

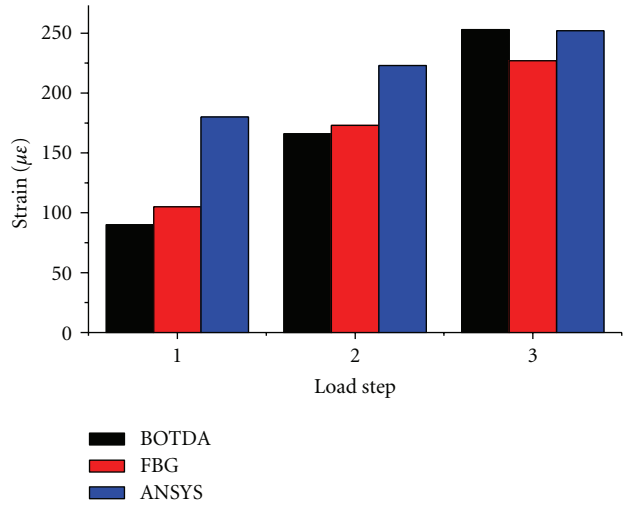

Figure 21: Contrast of across-tension zone strain.

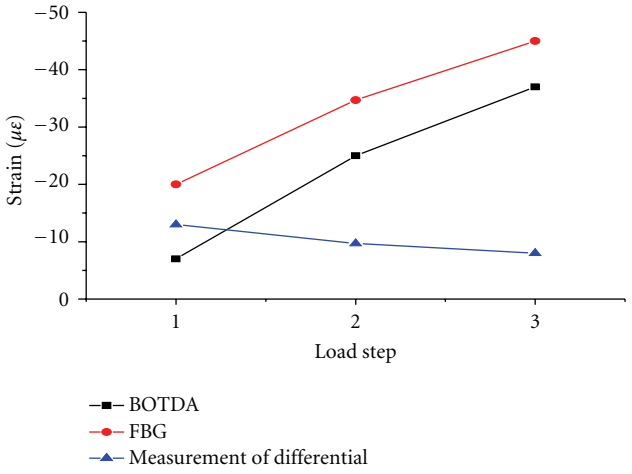

Figure 22: Contrast of across-pressure zone strain.

local structure, and focus on critical points. The combination of the distributed monitoring technology and the multiscale monitoring of fiber Bragg grating can obtain full information with local high precision and distributed high precision. The combination of these two methods can build more economical and reasonable multiscale sensor networks.

Acknowledgments

The authors thankful for the financial supports of the National Basic Research Program of China (2011CB013702), Key Projects in the National Science & Technology Pillar Program during the Twelfth Five-Year Plan Period (2011BAK02B02), and the National Natural Science Foundation of China (5092100).

References

[1] H.-N. Li, T.-H. Yi, X.-D. Yi, and G.-X. Wang, "Measurement and analysis of wind-induced response of tall building based on GPS technology," *Advances in Structural Engineering*, vol. 10, no. 1, pp. 83–93, 2007.

[2] T.-H. Yi, H.-N. Li, and M. Gu, "Full-scale measurements of dynamic response of suspension bridge subjected to environmental loads using GPS technology," *Science China Technological Sciences*, vol. 53, no. 2, pp. 469–479, 2010.

[3] T.-H. Yi, H.-N. Li, and M. Gu, "Characterization and extraction of global positioning system multipath signals using an improved particle-filtering algorithm," *Measurement Science and Technology*, vol. 22, no. 7, Article ID 075101, 2011.

[4] T.-H. Yi, H.-N. Li, and M. Gu, "Effect of different construction materials on propagation of GPS monitoring signals," *Measurement*, vol. 45, no. 5, pp. 1126–1139, 2012.

[5] Y. Xuan, Y. Liu, Q. Shi, and Q. Meng, "Experimental study of monitoring corrosion of steel bars using BOTDA," *Journal of Highway and Transportation Research and Development*, vol. 26, no. 11, pp. 82–86, 2009.

[6] Z. Qian, W. Huang, Y. Guan, and G. Han, "Application of BOTDA on cracking monitoring for asphalt concrete pavement," *Journal of Southeast University*, vol. 38, no. 5, pp. 799–803, 2008.

[7] Y. He, F. Xing, J.-H. Mao, and W.-L. Jin, "Study on real-time reinforcement stress measurement based on Brillouin optical time domain analysis," *Journal of Shenzhen University Science and Engineering*, vol. 27, no. 3, pp. 291–295, 2010.

[8] M. Sun, *Health monitoring of engineering structures using fiber bragg grating sensing technology [Ph.D. thesis]*, Sichuan University, Sichuan, China, 2005.

[9] J.-H. Huang and Y. Zhao, "Progress in strain measurement with fiber grating sensor," *Journal of Optoelectronics—Laser*, vol. 11, no. 2, pp. 216–220, 2000.

[10] T. Kurashima and M. Sato, "Measurement of strain distribution instructures using optical fiber," *JSCE*, vol. 82, pp. 18–20, 1997.

[11] Z. S. Wu, T. Takahashi, and K. Sudou, "An experimental investigation on continuous strain and crack monitoring with fiber optic sensors," *Concrete Research and Technology*, vol. 13, no. 2, pp. 139–148, 2002.

[12] D. Liu, *Study on long distance brillouin distributed optical fiber sensor [Ph.D. thesis]*, Zhejiang University, Zhejiang, China, 2005.